IL-21R blockade reduces inflammation and atherosclerosis in LDL receptor deficient mice

Snijckers, R.P.M.; Smit, V.; Postel, R.J.; Depuydt, M.A.C.; Bernabé Kleijn, M.N.A.; Bot, I.; ... ; Foks, A.C.

Atherosclerosis 421 (2026) 121899

Contents lists available at ScienceDirect

Atherosclerosis

journal homepage: www.elsevier.com/locate/atherosclerosis

IL-21R blockade reduces inflammation and atherosclerosis in LDL receptor deficient mice

Roy P.M. Snijckers, Virginia Smit, Rimke J. Postel, Marie A.C. Depuydt, Mireia N.A. Bernabé Kleijn, Ilze Bot, Jill de Mol, Amanda C. Foks *

Division of BioTherapeutics, Leiden Academic Centre for Drug Research, Leiden University, Einsteinweg 55, Leiden, 2333 CC, the Netherlands

HIGHLIGHTS

- The IL-21/IL-21R signaling pathway emerges as a potential anti-atherosclerosis therapeutic target.
- Age-related *Il21/Il21r* upregulation highlights relevance for CVD patients of advanced age.
- IL-21R blockade promotes atheroprotective Tregs and IL-10 and reduces pro-inflammatory myeloid cells in *Ldlr*$^{-/-}$ mice.
- Targeting IL-21R suppresses vascular inflammation and plaque development in *Ldlr*$^{-/-}$ mice.
- IL-21R blockade inhibits Tfh-B cell accumulation in aged *Ldlr*$^{-/-}$ mice.

GRAPHICAL ABSTRACT

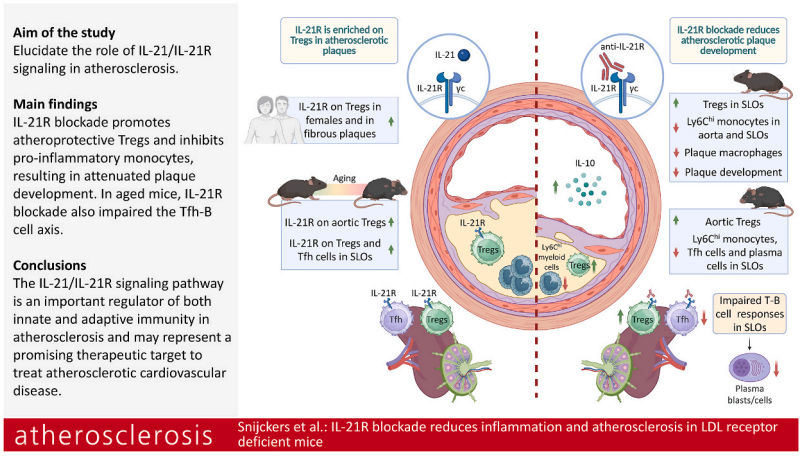

ARTICLE INFO

Keywords:
Atherosclerosis
Inflammation
Immunosenescence
Cytokines
IL-21

ABSTRACT

Background: Interleukin-21 (IL-21) is a pro-inflammatory cytokine involved in the regulation of both innate and adaptive immune responses and has been associated with atherosclerotic cardiovascular disease (ASCVD). However, the exact role of IL-21/IL-21R signaling in atherosclerosis and the therapeutic potential of targeting this axis remain unclear.

Methods and results: scRNAseq of human carotid plaques revealed that IL-21R is highly expressed on Tregs, with increased levels in women versus men and in fibrous plaques versus other phenotypes. In line with these findings, we showed that IL-21R blockade using an anti-IL-21R monoclonal antibody in young (20 weeks) *Ldlr*$^{-/-}$ mice increased Treg frequencies in secondary lymphoid organs (SLOs), accompanied by increased serum IL-10. Moreover, we observed reduced pro-inflammatory monocytes in the aorta and spleen of anti-IL-21R-treated mice. This contributed to a reduction of 38% in atherosclerotic plaque area ($p < 0.05$) and 61% less macrophage content ($p = 0.053$) upon IL-21R blockade. Furthermore, scRNAseq analysis of the spleen and aorta of female *Ldlr*$^{-/-}$ mice demonstrated an age-associated increase in *Il21/Il21r* expression within Tregs and Tfh cells.

* Corresponding author. Division of BioTherapeutics Leiden University, LACDR Einsteinweg 55, 2333CC, Leiden, the Netherlands
E-mail address: a.c.foks@lacdr.leidenuniv.nl (A.C. Foks).

https://doi.org/10.1016/j.atherosclerosis.2026.121899
Received 17 March 2026; Received in revised form 17 August 2026; Accepted 25 August 2026
Available online 3 September 2026

Subsequent IL-21R blockade in aged (88 weeks) *Ldlr*$^{-/-}$ mice with well-established plaques reduced inflammation, as shown by an increase in aortic Tregs, elevated Foxp3 expression in Tregs from SLOs and reduced pro-inflammatory monocytes. Additionally, anti-IL-21R-treated aged mice showed reduced Tfh cells, as well as reduced plasmablasts and plasma cells.

Conclusions: Collectively, we show that IL-21R blockade attenuates plaque initiation, promotes atheroprotective Tregs, inhibits pro-inflammatory monocytes and impairs Tfh-B cell dynamics upon aging, representing a promising novel therapeutic strategy to combat ASCVD.

1. Introduction

Cardiovascular diseases (CVD) are the leading cause of death worldwide. The main underlying pathology of CVD is atherosclerosis, which is characterized by sub-endothelial retention of apolipoprotein B-containing lipoproteins, primarily low-density lipoprotein (LDL), within the arterial wall. The aggravation and oxidation of retained lipoproteins can result in the formation of oxidized LDL (oxLDL) and other pro-inflammatory lipid species [1]. Subsequent endothelial activation induced by these modified lipoproteins promotes leukocyte recruitment and sustained cytokine-driven immune responses leading to plaque formation and progression. Rupture of these atherosclerotic plaques can result in acute cardiovascular events such as a myocardial infarction or stroke [2]. While the current focus on lipid-lowering strategies reduce CVD risk, accumulating evidence shows that the immune system is a central determinant of disease progression [3]. As such, many pro-inflammatory cytokines, including interleukin (IL)-1β, IL-6 and TNFα, are increased in the atherosclerotic milieu and inhibition of such cytokines has beneficial effects on disease outcome [4–6]. This is exemplified by the CANTOS trial, in which IL-1β inhibition in CVD patients, mediated through treatment with the monoclonal antibody Canakinumab, resulted in reduced recurrent cardiovascular events [7]. These observations underscore the therapeutic potential of targeting specific pro-inflammatory cytokine pathways involved in atherosclerotic immunity.

Among such pathways, the IL-21/IL-21 receptor (IL-21R) axis has emerged as a potent modulator of adaptive immunity. IL-21 is a pleiotropic cytokine of the IL-2 family produced primarily by follicular helper T (Tfh) cells, Th17 cells, and NKT cells, which signals exclusively through IL-21R - γc heterodimers expressed broadly across lymphoid and myeloid populations [8–11]. IL-21/IL-21R signaling promotes the differentiation, proliferation and survival of multiple T cell subsets, including Tfh, Th17 and CD8$^+$ T cells, while it additionally enhances the cytokine production and cytotoxic function of NKT cells [9,12–14].

IL-21/IL-21R signaling has furthermore been shown to be essential for the upregulation of B cell lymphoma 6 (Bcl-6), the lineage defining transcription factor for both Tfh cells and germinal center (GC) B cells [15]. IL-21-dependent Bcl-6 expression promotes Tfh and B cell activation, the formation of germinal centers in secondary lymphoid organs (SLOs) such as the spleen, and the generation of antibody secretion cells (ASCs) [16]. Moreover, the IL-21/IL-21R axis stimulates both antibody class switching and affinity maturation resulting in improved antibody responses [17]. In contrast, IL-21 has been shown to reduce expression of the IL-2 receptor alpha in various T cell subsets [18,19] and can inhibit IL-2 production by effector cells, thereby impairing the generation and survival of regulatory T cells (Tregs) [20]. Due to its pleiotropic nature, IL-21 has been implicated in multiple autoimmune diseases, with elevated levels in the serum, synovial fluid and gut of patients suffering from systemic lupus erythematosus and rheumatoid arthritis compared to healthy controls [21,22]. Moreover, IL-21R blockade in preclinical models of both diseases ameliorated inflammation and pathogenic autoantibody production [23,24].

Previously, it was shown that IL-21 levels are increased in serum of patients suffering from coronary artery disease compared to healthy controls [25]. However, the exact role of IL-21/IL-21R signaling in atherosclerosis remains unclear. In this study, we therefore profiled IL-21/IL-21R expression in atherosclerotic plaques using single-cell transcriptomics and investigated the impact of IL-21/IL-21R blockade on inflammation and atherosclerosis in young and aged *Ldlr*$^{-/-}$ mice. We showed that IL-21R is prominently expressed by Tregs within human and mouse atherosclerotic plaques. Subsequent blockade of the IL-21/IL-21R pathway with a monoclonal antibody reduced atherosclerosis development in *Ldlr*$^{-/-}$ mice, with a concomitant decrease in macrophage content. Mechanistically, we showed that IL-21R blockade reduced inflammatory monocytes, induced atheroprotective Treg immunity, and impaired Tfh-B cell dynamics. Together, our findings identify IL-21R signaling as a key regulator of immune balance in atherosclerosis.

2. Materials and methods

2.1. Patient population and single cell RNA sequencing

Primary atherosclerotic plaques were obtained from 46 patients (26 male, 20 female) undergoing a carotid endarterectomy (CEA) procedure at the University Medical Center Utrecht (UMCU) as part of the ongoing Athero-Express Biobank Study (AE, www.atheroexpress.nl) [26]. Culprit lesions (~5 mm) were classified histologically as fibrous (n = 14), fibro-atheromatous (n = 11), atheromatous (n = 12), or non-assigned (n = 9). Ethical approval and informed consent were obtained in accordance with the Declaration of Helsinki. Single cells were obtained and processed for single-cell RNA sequencing (scRNAseq) as previously described [27].

2.2. Animals

Female low-density lipoprotein receptor-deficient mice (*Ldlr*$^{-/-}$) on a C57Bl/6J genetic background were bred in-house and kept under standard laboratory conditions with diet and water being provided *ad libitum*. All animal work was approved by the Animal Ethics Committee and the Animal Welfare Body of Leiden University. Experiments were performed in accordance with directive 2010/63/EU of the European Parliament on the protection of animals used for scientific purposes.

2.3. Single-cell RNA sequencing of murine aortic and splenic CD45$^+$ cells

Single-cell transcriptomic data from murine aortas were derived from the previously published dataset by Smit et al. [28] who integrated live CD45$^+$ cells sorted from chow diet (CD)-fed young (2 months old, n = 9) female *Ldlr*$^{-/-}$ mice processed by Cochain et al. [29] with sorted live CD45$^+$ cells from atherosclerotic Western-type diet (WTD)-fed young (4-5 months old; n = 29), and CD-fed aged (22 months old; n = 12) female *Ldlr*$^{-/-}$ mice before subsequently characterizing immune populations.

Splenic CD45$^+$ single-cell suspensions were isolated from CD-fed young (5 months, n = 7) and aged (21 months, n = 8) female *Ldlr*$^{-/-}$ mice. Single-cell suspensions were stained with Fixable Viability Dye-eFluor 780 and CD45-PE. Following doublet removal, live CD45$^+$ cells were sorted using a FACS Aria II SORP (BD Biosciences) and loaded onto a Chromium Single Cell Controller (10x Genomics) to generate single-cell gel bead-in-emulsions. ScRNA-seq libraries were prepared using the Next GEM Single Cell 5' Kit V2 (10x Genomics). Samples were

subsequently sequenced on an Illumina HiSeq2500 after which digital expression matrices were generated by de-multiplexing cellular barcodes and counting transcript unique molecular indices (UMIs) using a Cell Ranger v6.0 pipeline (10x Genomics). Digital expression matrices were analyzed using the R package Seurat (v4). Cluster annotation was performed based on differential gene expression using the Seurat function FindAllMarker() as well as canonical cell markers. T cell clusters were selected and filtered by thresholding for $Cd3e^{+}>0.3$, $Cd3d^{+}>0.3$, $Cd19^{+}<0.3$, $Cd79a^{+}<0.3$ and $Cd79b^{+}<0.3$ to exclude non-T cells. For comparisons within single positive $Cd4^{+}$ T cells, the T cell subclustering was thresholded on $Cd4^{+} > 0.3$ and $Cd8a^{+} < 0.3$.

2.4. In vivo IL-21R blockade

To investigate the effects of IL-21/IL-21R signaling on the initial stages of atherosclerotic plaque development, young female $Ldlr^{-/-}$ mice (8-12 weeks of age) were fed a WTD containing 0.25% cholesterol and 15% cocoa butter (Special Diet Services, Witham, Essex, UK) for a period of 5 weeks while simultaneously receiving treatment with either 200 μg IL-21R blocking antibody (n = 15, *InVivo*MAb anti-mouse IL-21R, Clone 4A9, #BE0258, BioXcell) or 200 μg isotype control (n = 15, *InVivo*MAb rat IgG2a, anti-trinitrophenol, Clone 2A3, #BE0089, BioXcell) three times a week intraperitoneally.

The effects of IL-21R blockade on well-established advanced plaques were investigated using aged female $Ldlr^{-/-}$ mice (77-82 weeks of age) kept on a standard CD both before and during treatment. Mice were again treated with either the 200 μg IL-21R blocking antibody (n = 14) or 200 μg isotype control (n = 15) for three times a week intraperitoneally for a period of 5 weeks.

In both studies, mice were randomized according to basal weight and cholesterol levels before treatment initiation. During the experiments, mice were weighed weekly and blood samples were obtained by tail vein bleeding at T = 0 and T = 2.5 weeks. At the end of both experiments, mice were terminally anaesthetized by subcutaneous injection of a cocktail containing ketamine (40 mg/mL), atropine (0.1 mg/mL) and sedazine (8 mg/mL). Mice were bled by retro-orbital bleeding followed by *in situ* perfusion with phosphate-buffered saline (PBS) through the left cardiac ventricle, after which tissues were collected.

2.5. Serum cholesterol measurements

Serum was acquired by centrifugation of blood samples at 8000 rpm at 4°C for 10 min and stored at −80°C until further use. Total cholesterol levels in serum were determined using enzymatic colorimetric procedures (Roche/Hitachi, Mannheim, Germany). Precipath (Roche/Hitachi, Mannheim, Germany) was used as an internal standard.

2.6. Flow cytometry

Blood, spleen, aortas, and heart-draining mediastinal lymph nodes (HLN) were collected and prepared into single-cell suspensions. Erythrocytes were lysed from blood samples with ACK lysis buffer (0.15 M NH_4Cl, 1 mM $KHCO_3$, 0.1 mM Na_2EDTA; pH 7.3). Spleens and HLN were mashed through 70 μm cell strainers (Greiner Bio-One), after which erythrocytes were removed from splenocyte suspensions with ACK lysis buffer. Aortas were digested for 30 min at 37°C with a digestion mix containing 450 U/mL Collagenase I, 250 U/mL Collagenase XI, 120 U/mL Hyaluronidase and 120 U/mL DNAse, after which single-cell suspensions were obtained with 70 μm cell strainers (Greiner Bio-One). Single-cell suspensions were blocked with TruStain FcX™ αCD16/32 Fc block (Biolegend) and extracellularly labelled using fluorochrome-conjugated antibodies for surface markers (Supplemental Table S1) and Fixable Viability Stain in FACS buffer (5% FBS in PBS). For intracellular staining, cells were fixed in fixation buffer and permeabilized in permeabilization buffer according to manufacturer's protocol (Invitrogen eBioscience Foxp3/Transcription Factor Staining Buffer Set) and subsequently labelled with fluorochrome-conjugated antibodies for intracellular markers (Supplemental Table S1). Labelled cells were detected by flow cytometry on a CytoFLEX S (Beckman Coulter) and analyzed with FlowJo Software v10 (Tree Star, inc.)

2.7. Histology

Hearts were embedded in O.C.T. (Sakura) and snap-frozen. To determine plaque size, cryosections (10 μm) of the aortic root were stained with Oil-Red-O (ORO) and hematoxylin (Sigma-Aldrich). The section with the largest lesion plus four flanking sections were analyzed for lesion size. For lesion composition the section with the largest lesion and two flanking sections were analyzed. Collagen content in the lesion was assessed with Masson's trichrome staining according to manufacturer's protocol (Sigma-Aldrich). Corresponding sections on separate slides were also stained for monocyte/macrophage content with a MOMA-2 antibody (1:1000, AbD Serotec) followed by a biotinylated goat anti-rat IgG antibody (1:200, Vector). Secondary antibodies were detected using the Vectastain ABC kit (Vector) and visualized with ImmPACT NovaRED HRP substrate (Vector). The relative amount of collagen and percentage of macrophage content in the lesions is expressed as the ratio between the collagen- or MOMA-2- positive and the total lesion surface area. ORO-stained slides were captured with a Mikrocam II (Besser) linked to a Leica DM6000 microscope and other slides were captured with a panoramic 250 Flash III slide scanner (3DHistech). Images were manually analyzed using Fiji (ImageJ software).

2.8. Cell culture

200,000 splenocytes isolated from young and aged female $Ldlr^{-/-}$ mice treated with the IL-21R blocking antibody (n = 15) or isotype control (n = 15) were cultured in triplicates for 3 days at 37°C, 5% CO_2 in complete RPMI 1640 medium containing 10% heat-inactivated FBS, 1% L-glutamine, 100 IU/mL penicillin and 100 μg/mL streptomycin) in 96-well U bottom plates, in the presence of 0.5 μg/mL soluble anti-CD3e (eBioscience, #14-0031-86) and 5 μg/mL soluble anti-CD28 (eBioscience, #14-0281-82). After 3 days, supernatant for cytokine analysis was collected and stored at −80°C.

2.9. Cytokine analysis

Cytokines in serum and supernatant of stimulated splenocytes were analyzed using the LEGENDplex Murine Th Cytokine Panel (12-plex) V03 (Biolegend, #741044) according to manufacturer's protocol. Cytokine production was detected with a CytoFLEX S (Beckman Coulter) and further analyzed using LEGENDplex software.

2.10. Statistics

All data are expressed as mean ± SEM. Data were tested for normal distributions using a Shapiro-Wilk test. Outliers were determined within normally distributed data using a Grubbs test ($\alpha = 0.05$). Normally distributed data were tested for significance using an unpaired two-tailed student's t-test while non-parametric data were tested for significance using a Mann-Whitney test. *P*-values of <0.05 were considered significant. Correlation was determined using Pearson correlation coefficients and significance was determined using linear regression analysis. All statistical analyses were performed using GraphPad Prism 10.

3. Results

3.1. IL21R expression is enriched within FOXP3$^+$ Tregs of human carotid atherosclerotic plaques

We first aimed to investigate the expression of the *IL21/IL21R* axis in human atherosclerotic plaques. For this purpose, we employed a previously obtained scRNAseq dataset of atherosclerotic plaques from 46 patients who had undergone a CEA (Fig. 1A) [27]. In this study, unsupervised clustering identified 20 transcriptionally distinct populations, representing major immune, stromal and vascular cell types (Fig. 1B). We analyzed *IL21* and *IL21R* expression amongst the cell clusters within this dataset. Although *IL21R* transcripts were detected across all clusters, expression was markedly increased in T cell clusters, whereas *IL21* showed low expression across clusters, as expected from cytokine transcription levels in unstimulated samples (Fig. 1C and D). *IL21R* expression was most prominently enriched within *FOXP3*$^+$ Tregs compared to other *CD4*$^+$ T cells (Fig. 1E). Additionally, stratification by sex suggests heightened *IL21R* expression in plaque-derived Tregs from females as compared to males (Fig. 1E). Moreover, variable levels of *IL21R* were observed dependent on plaque phenotype, with *FOXP3*$^+$ Tregs displaying elevated *IL21R* expression in fibrous plaques as compared to atheromatous or fibro-atheromatous lesions (Fig. 1F). Together, these data identify Tregs as a dominant *IL21R*-expressing population in the human atherosclerotic environment, with expression influenced by sex and plaque phenotype.

3.2. IL-21R blockade reduces atherosclerotic plaque formation and promotes atheroprotective Tregs in young Ldlr$^{-/-}$ mice

As IL-21R is expressed in atherosclerotic plaques and IL-21/IL-21R signaling has a key role in driving adaptive immunity, we next investigated whether interference in this signaling pathway can affect atherosclerosis development. Young (8-12 weeks) female *Ldlr*$^{-/-}$ mice were fed a WTD and received triweekly intraperitoneal injections of either a monoclonal αIL-21R antibody (n = 15) or a rat IgG2a isotype control (n = 15) for a period of five weeks (Fig. 2A). Along the experimental timeline, treatment with the IL-21R blocking antibody did not affect total serum cholesterol levels or body weight and the effective targeting of IL-21R was confirmed upon sacrifice by flow cytometry (spleen, αIL-21R: 0.99 ± 0.18% of live CD45$^+$ vs Ctrl: 12.9 ± 3.68% of live CD45$^+$, $p < 0.0001$) (Fig. 2B–D). We observed that IL-21R blockade led to a 38% reduction in atherosclerotic plaque size in the three-valve area of the aortic root (αIL-21R: 0.72 ± 0.09 × 10^5 μm^2 vs ctrl: 1.15 ± 0.19 × 10^5 μm^2, $p < 0.05$), with a concomitant 61% decrease in plaque macrophage content (αIL-21R: 0.26 ± 0.07 × 10^5 μm^2 vs ctrl:

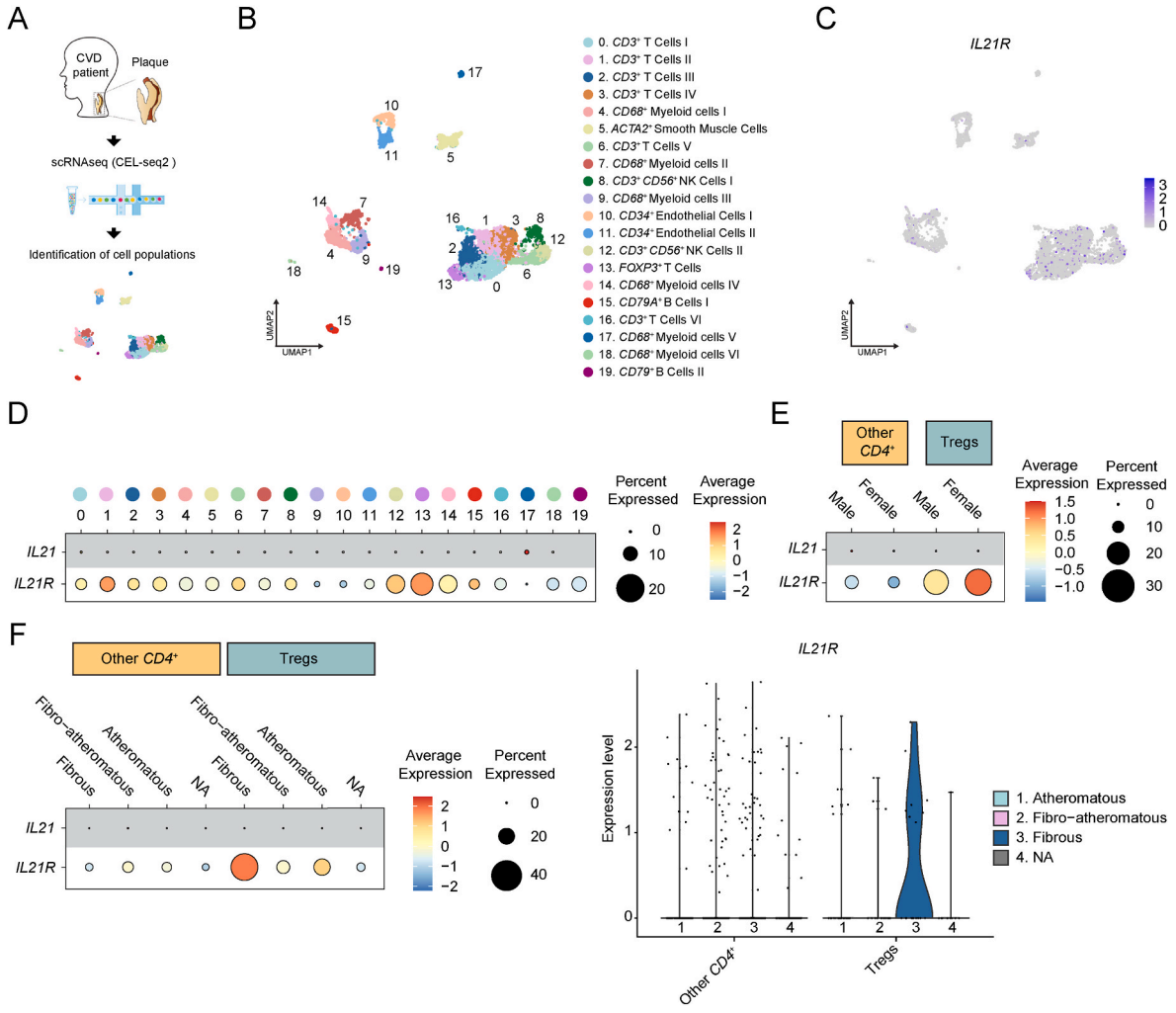

Fig. 1. scRNAseq of human carotid endarterectomy samples reveals *IL21R* expression in Tregs. (A) Experimental setup: carotid endarterectomy samples (N = 46) were digested and sorted for single viable cells using fluorescence-activated cell sorting (FACS) after which CEL-seq2 was performed as previously described [27]. **(B)** UMAP dim plot of sequenced cells shows 20 distinct populations. **(C)** Feature plot showing genetic expression of *IL21R*. **(D)** Relative gene expression of *IL21* and *IL21R* in all clusters. Dot plots showings the average expression of *IL21* and *Il21R* in the *FOXP3*$^+$ Treg cluster relative to all other *CD4*$^+$ T cells, split by **(E)** sex and **(F)** lesion phenotype (fibrous, fibro-atheromatous and atheromatous).

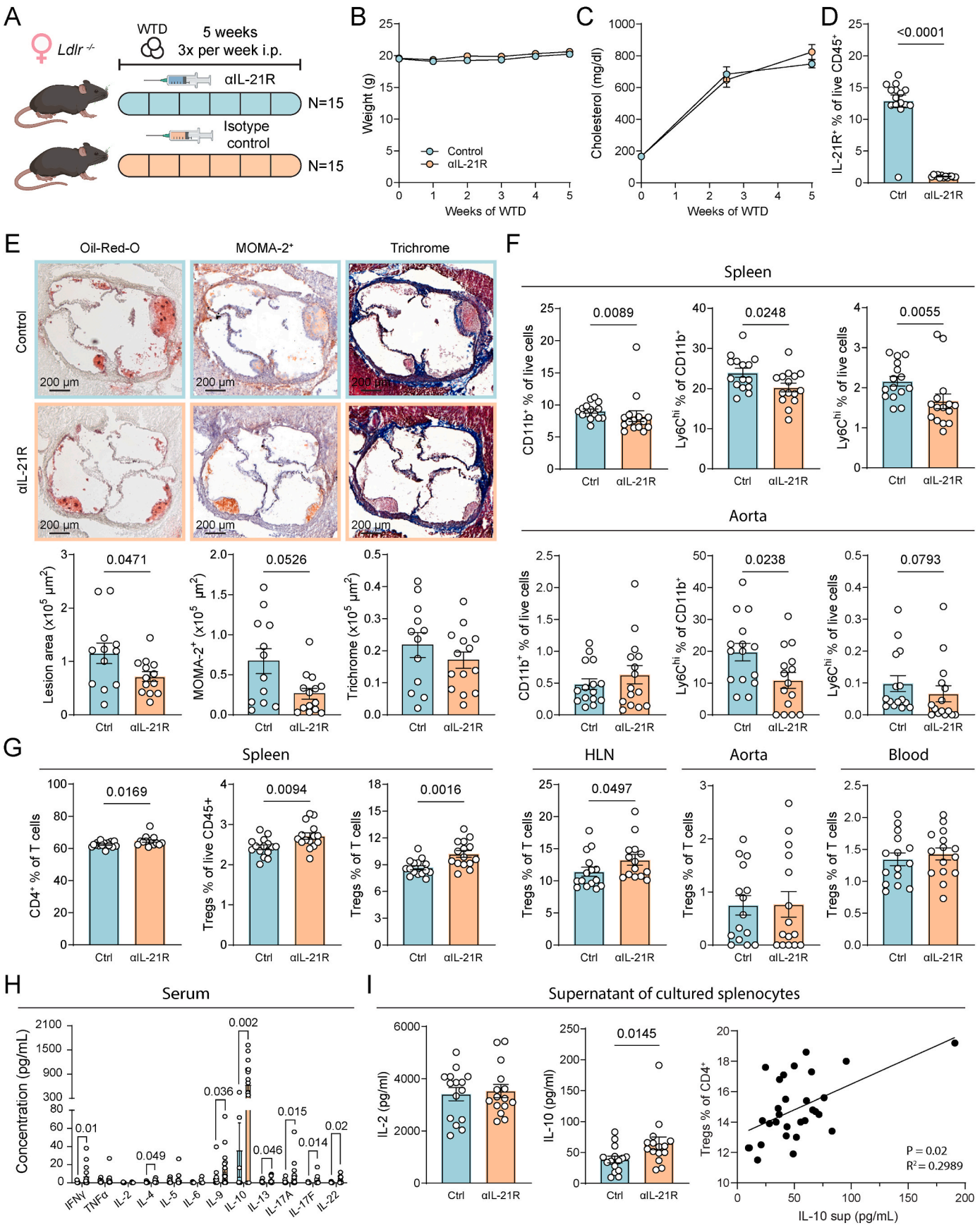

(caption on next page)

Fig. 2. IL-21R blockade reduces atherosclerotic plaque formation by promoting atheroprotective Tregs in young *Ldlr*$^{-/-}$ mice. (A) Experimental set-up: young (8-12 weeks) female *Ldlr*$^{-/-}$ mice fed a Western-type diet (WTD) to induce atherosclerosis were administered a triweekly intraperitoneal injection of an αIL-21R monoclonal antibody (αIL-21R) or isotype control (Ctrl) for a period of 5 weeks. During the experiment, both **(B)** body weight and **(C)** serum cholesterol levels were monitored. **(D)** After 5 weeks, the percentage of IL-21R-expressing cells in the spleen were measured by flow cytometry. **(E)** Lesion size, macrophage content and collagen content in the aortic three-valve area was histologically assessed by Oil-Red-O and hematoxylin staining, MOMA-2^{+} staining and Masson's trichome staining, respectively. Flow cytometry analysis showing **(F)** percentages of CD11b^{+} myeloid cells and Ly6C^{hi} monocytes within the spleen and aorta as well as **(G)** percentages of CD4^{+} T cells and Foxp3^{+} Tregs in the spleen, aorta, mediastinal lymph nodes (HLN) and blood following IL-21R blockade. Cytokine levels were analyzed using a LEGENDplex assay in both **(H)** serum samples and **(I)** supernatants of splenocytes restimulated *ex vivo* for 72h using αCD3/αCD28. Statistical significance was tested by two-tailed unpaired *t*-test for parametric data and Mann-Whitney test for non-parametric data. Data was obtained from n = 12-15 mice per group and plotted as mean ± SEM. (For interpretation of the references to color in this figure legend, the reader is referred to the Web version of this article.)

$0.67 \pm 0.16 \times 10^5$ μm^2, p = 0.053) (Fig. 2E). In line with these findings, we observed a local and systemic reduction of myeloid cells, in particular Ly6C^{hi} monocytes (Fig. 2F). Collagen deposition within lesions remained comparable between groups (Fig. 2E).

Furthermore, IL-21R blockade attenuated inflammation by promoting Foxp3^{+} Tregs in the spleen (αIL-21R: 10.21 ± 0.38% of T cells vs ctrl: 8.67 ± 0.23% of T cells, p < 0.01) and HLN (αIL-21R: 13.26 ± 0.84% of T cells vs ctrl: 11.42 ± 0.70% of T cells, p < 0.05), while overall CD4^{+} T cells were increased in the spleen (αIL-21R: 64.61 ± 0.79% of T cells vs ctrl: 62.40 ± 0.45% of T cells, p < 0.05) (Fig. 2G). Other T cell subsets such as Th1, Th2, Th17, follicular regulatory T (Tfr) and Tfh cells, as well as B cell subsets, plasma cells and plasmablasts were not altered upon IL-21R blockade (Figs. S1–2). Upon αIL-21R blockade, various cytokines, such as IFNy, IL-4, IL-9, IL-10, IL-13, IL-17 and IL-22 became significantly elevated in the serum, with anti-inflammatory IL-10 showing both the largest increase (17.8-fold) and the highest concentration (αIL-21R: 640.2 ± 147.8 pg/mL vs ctrl: 36.01 ± 29.93 pg/mL, p < 0.01) following treatment, which is consistent with the observed increase in Tregs (Fig. 2H). Similarly, splenocytes restimulated using αCD3/αCD28 *ex vivo* displayed increased production of IL-10 (αIL-21R: 64.86 ± 10.24 pg/mL vs ctrl: 38.58 ± 5.41 pg/mL, p < 0.05), which correlated to the amount of Tregs found within the spleens of the mice (Fig. 2I). Collectively, these data demonstrate that IL-21R blockade attenuated early plaque formation in young mice through the promotion of atheroprotective Tregs and the reduction in plaque monocyte/macrophage content.

3.3. Aging enhances *Il21* and *Il21r* expression within murine aortic and splenic T cell compartments

Given that ASCVD is largely a disease of aging [30], we next investigated the IL-21/IL-21R pathway in aged *Ldlr*$^{-/-}$ mice. This model reflects gradual plaque development under only mild hypercholesterolemia, a setting which resembles human disease progression [31]. Additionally, these mice possess an aged immune system, which is of particular interest in light of the age-associated increase in IL-21 production by PBMCs and CD4^{+} T cells reported in humans [32–34]. Aortic *Il21* and *Il21r* expression was investigated using our previously published scRNAseq datasets [28], containing sorted single live CD45^{+} cells from digested aortas of young versus aged *Ldlr*$^{-/-}$ mice (Fig. 3A). *Cd3e* $^{+}$ T cell subclustering identified 12 transcriptionally distinct populations (Fig. 3B). *Il21r* expression was detectable across multiple T cell subsets (Fig. 3C and D) and, in line with our human data (Fig. 1), was markedly elevated within aortic *Foxp3*$^{+}$ Tregs of aged mice as compared to other *Cd4*$^{+}$ T cells (Fig. 3E). Similarly, *Il21* transcripts showed age-associated increases within *Foxp3*$^{+}$ Tregs of aged mice as compared to their younger counterparts (Fig. 3E). In the spleen, scRNAseq analysis of sorted single live CD45^{+} cells from CD fed young (5 months) and aged (21 months) female *Ldlr*$^{-/-}$ mice, identified 12 clusters within the *Cd3e* $^{+}$ *Cd3d* $^{+}$ T cell subclustering (Fig. 3F and G). Here, splenic *Foxp3*$^{+}$ Tregs and *Cxcr5*$^{+}$ *Bcl6*$^{+}$ Tfh cells represented the main *Il21*-and *Il21r* expressing subsets (Fig. 3H and I). Additionally, both *Foxp3*$^{+}$ Tregs and *Cxcr5*$^{+}$ *Bcl6*$^{+}$ Tfh cells displayed an age-associated upregulation of *Il21r* compared to other *Cd4*$^{+}$ T cells. Moreover, the Tfh cluster exhibited an age-associated increase in *Il21* expression (Fig. 3J). These findings indicate that aging amplifies the *Il21/Il21r* axis within aortic and splenic T cell subsets, specifically in those involved in Tfh-B cell interactions as well as in Tregs.

3.4. Tregs are increased by IL-21R blockade in aged *Ldlr*$^{-/-}$ mice

To determine whether blocking of the IL-21/IL-21R axis can modulate immune responses in aged mice with well-established atherosclerotic plaques, we treated aged female *Ldlr*$^{-/-}$ mice with the αIL-21R monoclonal antibody (n = 15) or isotype control (n = 15) intraperitoneally three times a week for a period of five weeks (Fig. 4A). Similar to the treatment in young mice, body weight and cholesterol levels remained unaffected during the experimental timeline (Fig. 4B and C). Additionally, antibody efficacy was confirmed by reduced IL-21R levels at the time of sacrifice (αIL-21R: 0.28 ± 0.03% of live CD45^{+} vs ctrl: 34.23 ± 4.47% of live CD45^{+}, p < 0.0001) (Fig. 4D). In contrast to young mice, plaque size and composition was not altered in aged mice following 5 weeks of IL-21R blockade (Fig. 4E). We did observe a trend towards reduced myeloid cells in the spleen (αIL-21R: 8.43 ± 1.36% of live cells vs ctrl: 9.02 ± 0.33% of live cells, p = 0.06), with a significant decrease of Ly6C^{hi} monocytes (αIL-21R: 1.32 ± 0.13% of live cells vs ctrl: 1.81 ± 0.14% of live cells, p < 0.05) (Fig. 4F). Moreover, IL-21R blockade significantly increased the frequency of aortic Foxp3^{+} Tregs within the CD4^{+} T cell compartment (αIL-21R: 12.95 ± 1.42% vs ctrl: 8.84 ± 1.31%, p < 0.05) and increased the mean fluorescence intensity (MFI) of the proliferation marker Ki67 within aortic Tregs as well (Fig. 4G). Similarly, IL-21R blockade elevated Foxp3 MFI within Tregs from SLOs, such as the spleen (αIL-21R: 16552 ± 362.1 vs ctrl:15795 ± 149.5, p < 0.01) and HLN (αIL-21R: 23284 ± 389.9 vs ctrl: 21411 ± 290.3, p < 0.001) (Fig. 4G).No differences were observed in serum IL-10 levels or in the supernatant of splenocytes which were restimulated *ex vivo* using αCD3/αCD28 (Fig. S3A–B).

3.5. IL-21R blockade attenuates the pro-atherogenic Tfh-B cell axis in aged *Ldlr*$^{-/-}$ mice

Given the importance of the IL-21/IL-21R signaling axis in Tfh-B cell communication in SLOs [17], we next examined whether IL-21R blockade affects the Tfh-B cell axis in aged *Ldlr*$^{-/-}$ mice. Flow cytometry revealed reduced frequencies of Foxp3^{-} CXCR5^{+} Bcl-6^{+} Tfh cells in the spleen (αIL-21R: 0.61 ± 0.06% of live cells vs ctrl: 0.89 ± 0.08% of live cells, p < 0.01) and HLN (αIL-21R: 1.10 ± 0.10% of live cells vs ctrl: 1.53 ± 0.18% of live cells, p < 0.05) whilst Foxp3^{+} CXCR5^{+} Bcl-6^{+} Tfr cell levels remained unaffected, driving a shift towards a more atheroprotective Tfh/Tfr ratio (Fig. 5A). In parallel, following IL-21R inhibition, trends were observed towards increased follicular (FO) B cell proportions, without impacting marginal zone (MZ) B cells (Fig. 5B). Moreover, αIL-21R treatment in aged mice resulted in a trend towards reduced frequencies of age-associated B cells (ABCs) in HLNs (αIL-21R: 18.46 ± 2.00% of B cells vs ctrl: 21.22 ± 1.34% of B cells, p = 0.07). The percentage of pro-inflammatory T-bet^{+} within ABCs was significantly diminished in both the spleen (αIL-21R: 51.66 ± 5.71% vs ctrl: 68.66 ± 3.00% p < 0.05) and HLN (αIL-21R: 24.17 ± 2.41% vs ctrl: 32.83 ± 2.67%, p < 0.05) (Fig. 5B). Additionally, CD138^{+} B220^{+} plasmablasts and CD138^{+} B220^{-} plasma cells were reduced in both the

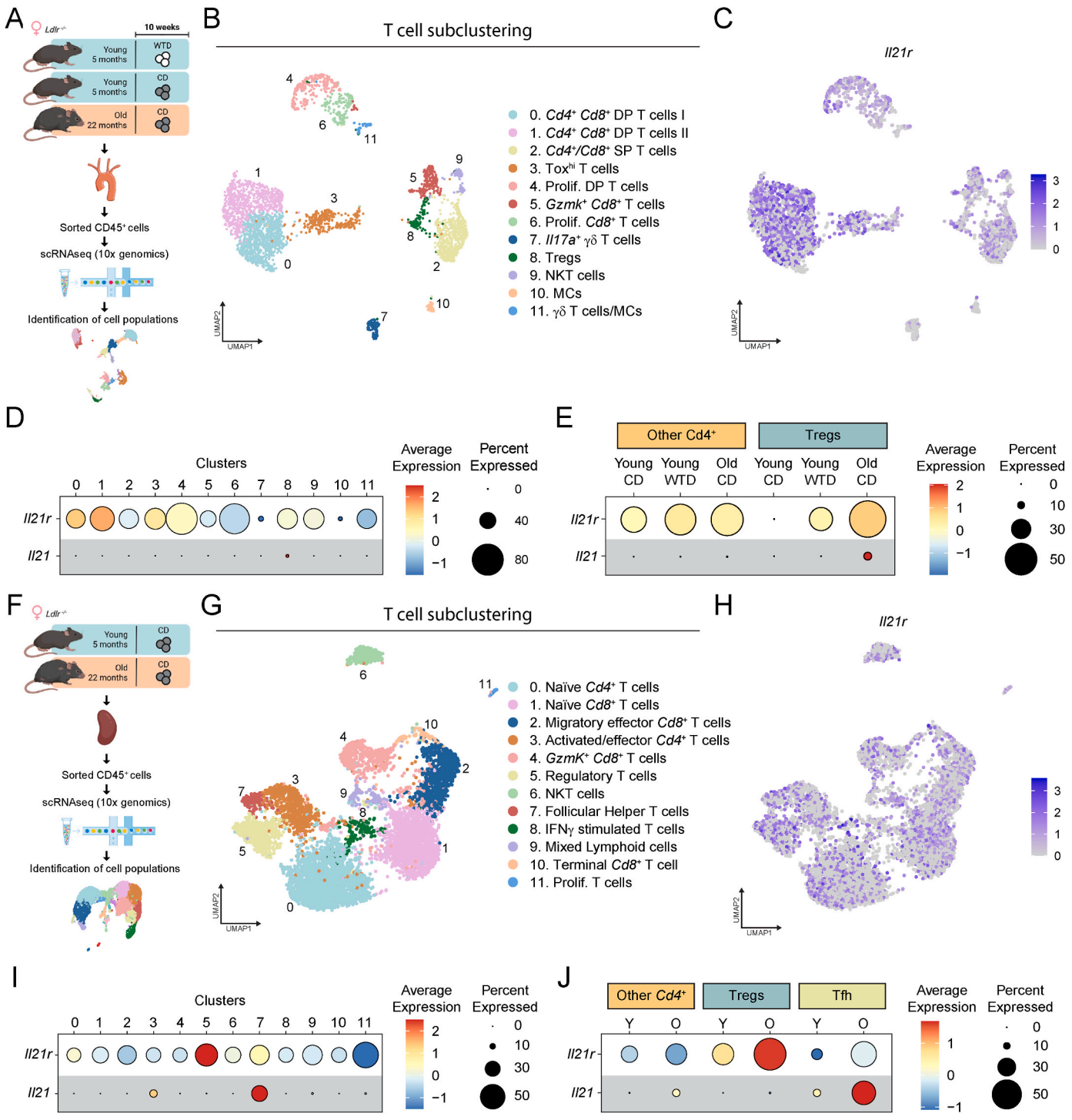

Fig. 3. scRNAseq demonstrates an age-associated increase of *Il21* and *Il21r* expression in the aorta and spleen. (A) Experimental set-up: single-cell RNA-sequencing of CD45$^+$ immune cells sorted from digested aortas obtained from young (16-20 weeks) female *Ldlr*$^{-/-}$ mice fed either a chow diet (CD) (n = 9) or Western type diet (WTD) (n = 29) and aged (88 weeks) female *Ldlr*$^{-/-}$ mice fed a CD (n = 12). **(B)** UMAP dim plot of *Cd3e* $^+$ T cell subclustering identified 12 distinct populations. **(C)** Genetic expression of *Il21r* projected onto the aortic T cell subclustering UMAP. **(D)** Dot plot showing the relative gene expression of *Il21* and *Il21r* in all clusters. **(E)** Average expression of *Il21* and *Il21r* in the *Foxp3*$^+$ Treg cluster relative to all other *Cd4*$^+$ cells, split by age and diet. **(F)** Experimental set-up: single-cell RNA-sequencing of CD45$^+$ immune cells sorted from spleens obtained from young (20 weeks, n = 7) or aged (84 weeks, n = 8) female *Ldlr*$^{-/-}$ mice fed a CD. **(G)** UMAP dim plot of *Cd3e* $^+$ *Cd3d* $^+$ T cell subclustering identified 12 distinct populations. **(H)** Genetic expression of *Il21r* projected unto the splenic T cell subclustering UMAP. **(I)** Relative gene expression of *Il21* and *Il21r* in all clusters. **(J)** Average expression of *Il21* and *Il21r* in the *Foxp3*$^+$ Treg cluster and *Cxcr5*$^+$ *Bcl6*$^+$ follicular T helper cell cluster relative to all other *Cd4*$^+$ cells, split by age.

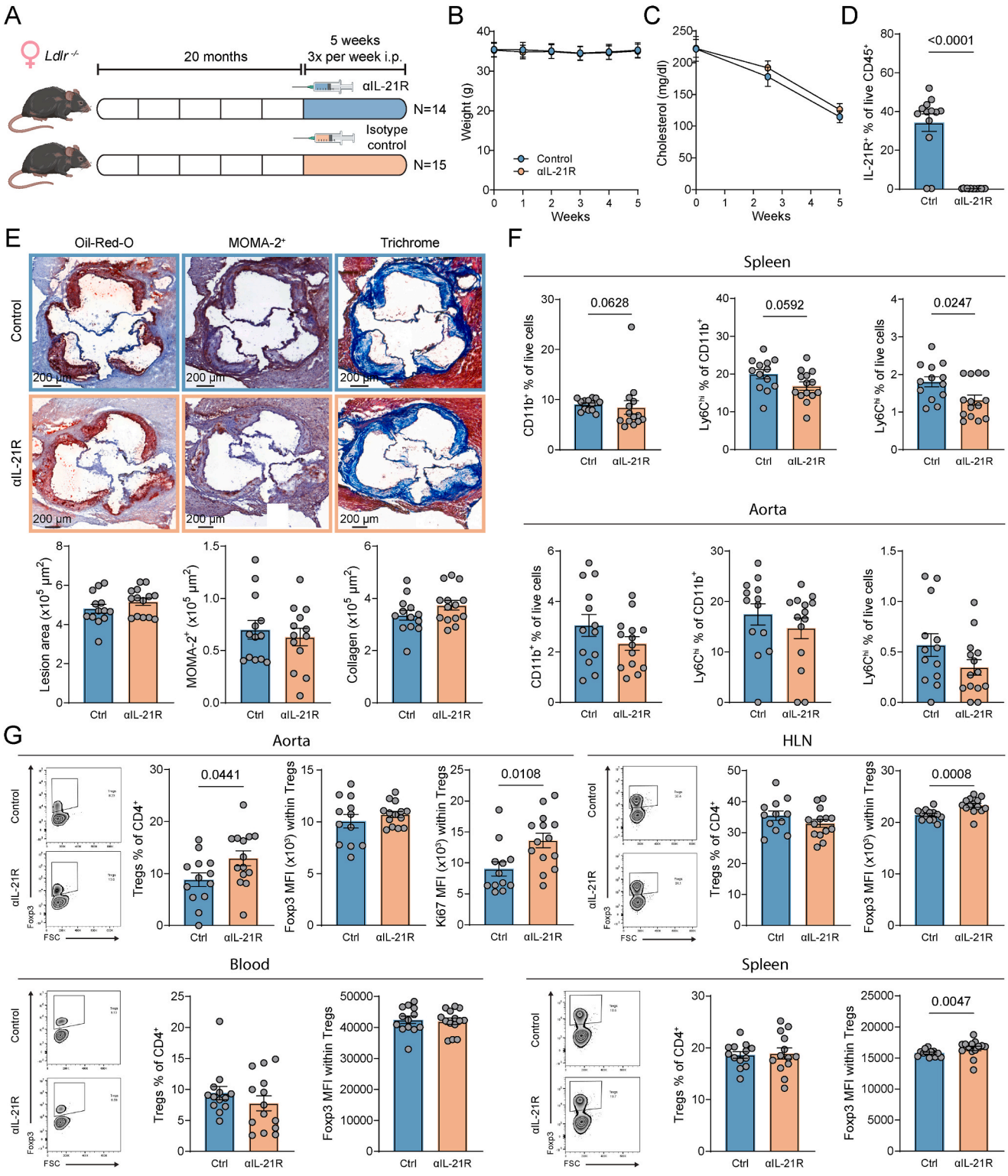

Fig. 4. Tregs are increased by IL-21R blockade in aged *Ldlr*$^{-/-}$ mice. (A) Experimental set-up: aged (77-82 weeks) female *Ldlr*$^{-/-}$ mice maintained on a chow diet (CD) were administered a triweekly intraperitoneal injection of an αIL-21R monoclonal antibody (αIL-21R) or isotype control (Ctrl) for a period of 5 weeks. During the experiment, both **(B)** weight and **(C)** serum cholesterol levels were monitored. **(D)** After 5 weeks, IL-21R^{+} levels in the spleen were measured via flow cytometry. **(E)** Lesion size, monocyte/macrophage content and collagen content in the aortic three-valve area was histologically assessed by Oil-Red-O and hematoxylin staining, MOMA-2^{+} staining and Masson's trichome staining, respectively. Flow cytometry analysis quantification following IL-21R blockade of **(F)** percentage of CD11b^{+} myeloid cells and Ly6C^{hi} monocytes within the spleen and aorta as well as **(G)** percentages of Foxp3^{+} Tregs and Foxp3 MFI within Tregs of the aorta, mediastinal lymph nodes (HLN), blood and spleen as well as Ki67 MFI within aortic Tregs. Statistical significance was tested by two-tailed unpaired *t*-test for parametric data and Mann-Whitney test for non-parametric data. Data was obtained from n = 13-14 mice per group and plotted as mean ± SEM. (For interpretation of the references to color in this figure legend, the reader is referred to the Web version of this article.)

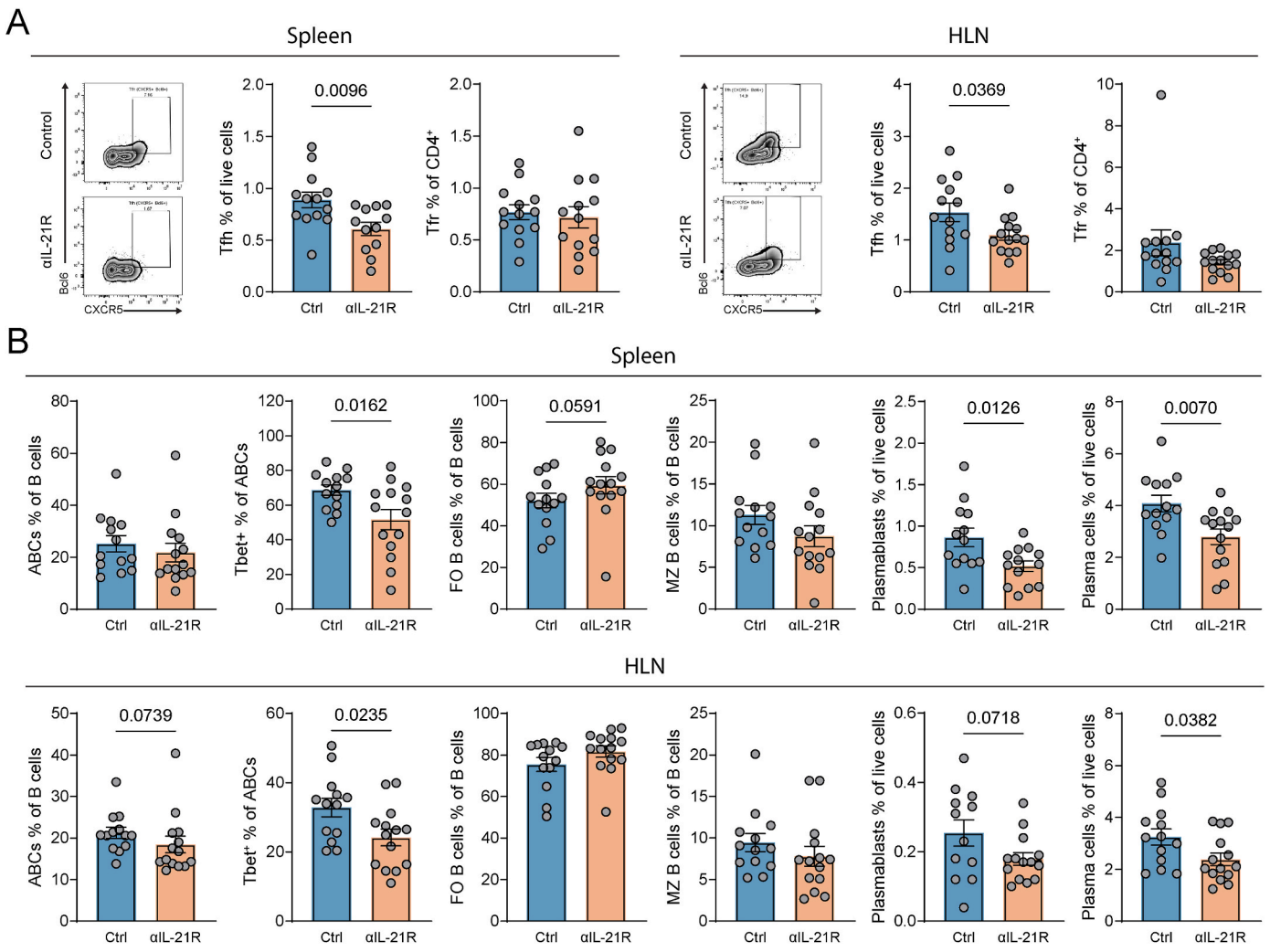

Fig. 5. IL-21R blockade attenuates the Tfh-B cell axis in SLOs of aged *Ldlr*$^{-/-}$ mice. Flow cytometry analysis of spleen and mediastinal lymph nodes (HLN) from aged (77-82 weeks) female *Ldlr*$^{-/-}$ mice showing **(A)** the percentage of Foxp3^{-} CXCR5^{+} Bcl-6^{+} follicular T helper cells and Foxp3^{+} CXCR5^{+} Bcl-6^{+} follicular T regulatory cells, as well as **(B)** B cell subsets, given the importance of IL-21/IL-21R signaling in Tfh-B cell communication, showing percentages of CD11b^{+}/CD11c^{+} age-associated B cells (ABCs), levels of T-bet^{+} within ABCs, CD21^{int} CD23^{+} follicular (FO) B cells, CD21^{+} CD23^{-} marginal zone (MZ) B cells, CD138^{+} B220^{+} plasmablasts and CD138^{+} B220^{-} plasma cells. Statistical significance was tested by two-tailed unpaired *t*-test for parametric data and Mann-Whitney test for non-parametric data. Data was obtained from n = 13-14 mice per group and plotted as mean ± SEM.

spleen and HLN (Fig. 5B). However, IL-21R blockade did not significantly alter circulating immunoglobulin levels or IgG/IgM deposition within atherosclerotic lesions (Fig. S4A–B). Taken together, these results indicate that IL-21R blockade disrupts the aged Tfh-B cell axis, leading to a reduction in plasmablasts and plasma cells.

4. Discussion

Over the past years, several studies have pointed out that targeting the over-active immune response can be beneficial in reducing cardiovascular disease [35–37]. The recent CANTOS trial demonstrated that neutralization of the pro-inflammatory cytokine IL-1β significantly reduced the risk of cardiovascular events [7] and IL-6 blocking using Ziltivekimab attenuated systemic inflammation in patients at high atherosclerotic risk [38]. In our study, we evaluated the IL-21/IL-21R axis as a potential immunomodulatory target in atherosclerosis using single-cell transcriptomics and *in vivo* IL-21R blockade in young and aged *Ldlr*$^{-/-}$ mice.

We show high *IL21R* expression on Tregs in carotid plaque samples obtained from ASCVD patients, demonstrating the clinical relevance of IL-21/IL-21R signaling. Additionally, transcriptome analyses at the single cell level suggests increased *IL21R* expression in Tregs from fibrous plaques compared to other phenotypes as well as in Tregs from women compared to men. In relation to sex dependent expression of *IL21R* on Tregs, both estrogen and progesterone have been reported to promote Treg generation and stability [39,40] as well as Tfh differentiation, whereas estrogen has also been shown to increase IL-21 production by Tfh cells in vitro [41]. Moreover, elevated *Il21* expression has already been observed in aortic T cells from female *Ldlr*$^{-/-}$ mice as compared to males [31]. As such, it stands to reason that sexual dimorphism could similarly contribute to the differential expression of *IL21R* in atherosclerosis. In line with high *IL21R* expression on Tregs in human plaques, murine scRNAseq revealed high *Il21 and Il21r* expression in Tregs and Tfh cells from atherosclerotic mice, which are further increased upon aging. These findings indicate that aging reinforces IL-21/IL-21R signaling, which could potentially stimulate both Tfh-driven humoral responses and IL-21-mediated modulation of Tregs in advanced disease.

Upon blockade of IL-21R, we observed an increased percentage of Tregs in both young and aged atherosclerotic mice, which is in line with previous studies demonstrating an increased percentage of Tregs upon genetic deficiency or therapeutic blockade of IL21/IL21R in mouse

inflammatory and transplant models [19,42–44] as well as in humans with *IL21R* loss of function mutations [19]. We hypothesize that IL-21R blockade directly promotes Treg expansion by preventing STAT3-mediated inhibition of *Foxp3* stability, independently of IL-2 availability [45–51]. Multiple preclinical studies have highlighted the atheroprotective role of Tregs [52–55]. Depletion of $CD4^+Foxp3^+$ T cells increased atherosclerosis development [52], while transfer experiments with $CD4^+Foxp3^+$ Tregs [53] or $CD4^+CD25^+$ Treg-like cells [54], as well as IL-2 complex-mediated expansion of Tregs [55], reduced atherosclerosis. Recently, low-dose IL-2 mediated Treg expansion decreased arterial inflammation in the IVORY trial and the IVORY-FINALE follow-up trial showed promising early evidence of reducing major adverse cardiovascular events in patients with acute coronary syndromes [56]. Elevated Treg immunity may additionally contribute to the observed reduction in pro-inflammatory myeloid cells upon IL-21R blockade as Tregs have been reported to inhibit myeloid cell activation and adhesion either through cell-cell mediated interactions or through the secretion of cytokines, including IL-10 [57–59]. Consistent with this notion, anti-IL-21R treatment increased systemic IL-10 levels in young mice, which correlated with splenic Treg abundance. Although IL-21R blockade did not increase systemic IL-10 levels in aged mice, it markedly increased aortic Tregs, suggesting local immunosuppression within the plaque. Additionally, given the age-associated upregulation of *Tgfb1* and *Ebi3* (IL-35) in aortic Tregs [28], these cytokines could contribute more strongly to the immunosuppressive capacity of aged Tregs as opposed to IL-10. Taken together, these findings suggest that Treg expansion may contribute to the observed attenuation of atherosclerosis development.

In addition to promoting Treg responses, IL-21R blockade markedly reduced pro-inflammatory myeloid cells in the aorta and spleen of atherosclerotic $Ldlr^{-/-}$ mice. Given the established role of pro-inflammatory monocytes and macrophages in plaque development, progression and inflammation [60,61], this reduction may represent an important mechanism underlying the attenuated atherosclerosis observed following treatment. Indeed, IL-21 has been reported to directly regulate myeloid cell function by enhancing monocyte adhesion to endothelial cells and carotid arteries through Syk activation [62], promoting macrophage phagocytic activity and increasing metalloproteinase-9 secretion [62,63]. Furthermore, local delivery of IL-21 has been reported to induce a shift in tumor-associated macrophages from an M2-like to a pro-inflammatory M1-like phenotype [64]. Therefore, inhibition of IL-21 signaling may have directly led to the reduction of pro-inflammatory myeloid cells observed in our study.

Moreover, we observed decreased Tfh cells, plasmablast and plasma cells in anti-IL-21R treated mice compared to control mice, which is consistent with the well-established role of IL-21 as a key driver of germinal center responses [15,17]. However, both circulating immunoglobulin levels and IgG/IgM deposition within atherosclerotic lesions remained unaltered in aged mice upon IL-21R blockade. Notably, mice were treated for a short period of time (5 weeks) and it can be argued that more time is needed for the observed reduction of the Tfh-B cell axis to translate into altered immunoglobulin levels. IL-21R blockade additionally reduced pro-inflammatory T-bet in ABCs from SLOs while a trend was observed towards an overall reduction in ABCs [28]. These reductions are most likely mediated through both the direct blocking of IL-21R on ABCs as well as the reduction in Tfh cells upon anti-IL-21R treatment, as IL-21 is essential for ABC differentiation and T-bet expression [65,66]. Previously, ABCs have been shown to accumulate in an aging- and CVD-dependent manner and exhibit enhanced antigen-presenting capacity and pro-inflammatory cytokine expression [28]. The reduction of T-bet within ABCs likely reflects impaired pro-inflammatory signaling, thereby limiting their support of pro-atherogenic adaptive immune responses.

While plaque size was significantly reduced in young mice, IL-21R blockade did not alter lesion size or composition in aged mice with established atherosclerosis. This likely reflects fundamental differences in anti-inflammatory treatment at the start of plaque development versus interference at an advanced disease stage where the treatment period relative to the time-of-development of atherosclerosis is significantly smaller. In addition to intervening in atherosclerotic plaque development at an earlier timepoint, it may be that a longer IL-21R-blockade treatment would be required for the observed immunomodulatory effects to translate to a reduction in lesion size or plaque vulnerability. This is especially true given evidence suggesting that Tregs may contribute to plaque stabilization and resolution of vascular inflammation. Previous studies revealed that human carotid endarterectomy specimens show an inverse correlation between stability and Treg numbers both through immunohistochemical staining and PCR analysis [48] and the amount of collagen content and plaque stability was likewise increased upon Treg expansion by IL-2 complex [55]. Similarly, IL-10 has been linked to plaque stability by driving a reduction in necrotic core size [67], while IL-10 deficient mice exhibit decreased plaque collagen content [68] as well as increased proteolytic and procoagulant activity [69]. Several aspects have to be considered with a prolonged IL-21R blockade and its potential consequences for protective immunity. Life time deficiencies in *Il21r* knock-out mice have demonstrated impaired germinal center responses, plasma cell differentiation and immunoglobulin class switching [17,70,71], while patients with loss-of-function mutations in *IL21R* exhibit defective antibody responses and increased susceptibility to recurrent infections [72]. Regardless, clinical studies using the anti-IL-21 monoclonal antibodies NNC0114-0005 [73] in rheumatoid arthritis patients and BOS161721 [74] in healthy volunteers demonstrated acceptable antibody safety and tolerability, with only mild adverse events reported, supporting the translational potential of this therapeutic approach while highlighting the need to monitor long-term effects on humoral immunity.

Collectively, we show that IL-21R blockade attenuates atherosclerosis development while promoting atheroprotective Treg immunity, reducing inflammatory myeloid cells and, in aged mice, suppressing the Tfh-B cell axis. Together, these findings identify IL-21/IL-21R signaling as an important regulator of both innate and adaptive immunity in atherosclerosis and highlight its potential as a therapeutic target.

Author contributions

R.P.M.S., R.J.*P. and* A.C.F participated in the conceptualization. R.P.M.S. and R.J.P. wrote the manuscript. R.P.M.S. performed data analysis and designed figures. A.C.F. and J.d.M. provided critical feedback on the manuscript. R.P.M.S., R.J.P., V.S., J.d.M., M.A.C.D., M.N.A.B.K., I.B. and A.C.F. performed experiments. A.C.F. and J.d.M. supervised the work and A.C.F. provided funding. All authors provided feedback on the research and analyses and agreed to the published version of the manuscript.

Financial support

This work was supported by the Dutch Heart Foundation (grant number 2018T051 to A.C.F., 2019T067 to I.B., and 03-006-2024-0122 to M.A.C.D.), Dutch Heart Foundation funded consortia ERA-CVD BeatATHERO (grant number 2019T107 to A.C.F) and Treat-ATHERO (grant number 02-001-2023-0138 to A.C.F), by the project 'B-specific' funded by the European Union under Grant Agreement No. 101115159, and the project MARGINALIZE-MI with file number era4healthcvd-105 of the research program ERA4Health CARDINNOV which is (partly) financed by the Dutch Research Council (NWO).

Conflict of interest

The authors declare no competing interest.

Acknowledgments

We would like to thank Eva Lievaart for her technical assistance. The graphical abstract for this manuscript was created using Biorender.com.

Appendix A. Supplementary data

Supplementary data to this article can be found online at https://doi.org/10.1016/j.atherosclerosis.2026.121899.

References

[1] Libby P. The changing landscape of atherosclerosis. Nature 2021;592(7855):524–33.
[2] Frostegard J. Immunity, atherosclerosis and cardiovascular disease. BMC Med 2013;11:117.
[3] Libby P, Lichtman AH, Hansson GK. Immune effector mechanisms implicated in atherosclerosis: from mice to humans. Immunity 2013;38(6):1092–104.
[4] Edsfeldt A, Grufman H, Asciutto G, Nitulescu M, Persson A, Nilsson M, et al. Circulating cytokines reflect the expression of pro-inflammatory cytokines in atherosclerotic plaques. Atherosclerosis 2015;241(2):443–9.
[5] Schuett H, Oestreich R, Waetzig GH, Annema W, Luchtefeld M, Hillmer A, et al. Transsignaling of interleukin-6 crucially contributes to atherosclerosis in mice. Arterioscler Thromb Vasc Biol 2012;32(2):281–90.
[6] Koga M, Kai H, Yasukawa H, Yamamoto T, Kawai Y, Kato S, et al. Inhibition of progression and stabilization of plaques by postnatal interferon-gamma function blocking in ApoE-knockout mice. Circ Res 2007;101(4):348–56.
[7] Ridker PM, Everett BM, Thuren T, MacFadyen JG, Chang WH, Ballantyne C, et al. Antiinflammatory therapy with canakinumab for atherosclerotic disease. N Engl J Med 2017;377(12):1119–31.
[8] Chtanova T, Tangye SG, Newton R, Frank N, Hodge MR, Rolph MS, Mackay CR. T follicular helper cells express a distinctive transcriptional profile, reflecting their role as non-Th1/Th2 effector cells that provide help for B cells. J Immunol 2004;173(1):68–78.
[9] Nurieva R, Yang XO, Martinez G, Zhang Y, Panopoulos AD, Ma L, et al. Essential autocrine regulation by IL-21 in the generation of inflammatory T cells. Nature 2007;448(7152):480–3.
[10] Coquet JM, Kyparissoudis K, Pellicci DG, Besra G, Berzins SP, Smyth MJ, Godfrey DI. IL-21 is produced by NKT cells and modulates NKT cell activation and cytokine production. J Immunol 2007;178(5):2827–34.
[11] Ozaki K, Kikly K, Michalovich D, Young PR, Leonard WJ. Cloning of a type I cytokine receptor most related to the IL-2 receptor beta chain. Proc Natl Acad Sci U S A 2000;97(21):11439–44.
[12] Vogelzang A, McGuire HM, Yu D, Sprent J, Mackay CR, King C. A fundamental role for interleukin-21 in the generation of T follicular helper cells. Immunity 2008;29(1):127–37.
[13] Brady J, Hayakawa Y, Smyth MJ, Nutt SL. IL-21 induces the functional maturation of murine NK cells. J Immunol 2004;172(4):2048–58.
[14] Zeng R, Spolski R, Finkelstein SE, Oh S, Kovanen PE, Hinrichs CS, et al. Synergy of IL-21 and IL-15 in regulating CD8+ T cell expansion and function. J Exp Med 2005;201(1):139–48.
[15] Linterman MA, Beaton L, Yu D, Ramiscal RR, Srivastava M, Hogan JJ, et al. IL-21 acts directly on B cells to regulate Bcl-6 expression and germinal center responses. J Exp Med 2010;207(2):353–63.
[16] Moens L, Tangye SG. Cytokine-Mediated regulation of plasma cell generation: IL-21 takes center stage. Front Immunol 2014;5:65.
[17] Ozaki K, Spolski R, Feng CG, Qi CF, Cheng J, Sher A, et al. A critical role for IL-21 in regulating immunoglobulin production. Science 2002;298(5598):1630–4.
[18] Hinrichs CS, Spolski R, Paulos CM, Gattinoni L, Kerstann KW, Palmer DC, et al. IL-2 and IL-21 confer opposing differentiation programs to CD8+ T cells for adoptive immunotherapy. Blood 2008;111(11):5326–33.
[19] Jandl C, Liu SM, Canete PF, Warren J, Hughes WE, Vogelzang A, et al. IL-21 restricts T follicular regulatory T cell proliferation through Bcl-6 mediated inhibition of responsiveness to IL-2. Nat Commun 2017;8(1):14647.
[20] Attridge K, Wang CJ, Wardzinski L, Kenefeck R, Chamberlain JL, Manzotti C, et al. IL-21 inhibits T cell IL-2 production and impairs treg homeostasis. Blood 2012;119(20):4656–64.
[21] Webb R, Merrill JT, Kelly JA, Sestak A, Kaufman KM, Langefeld CD, et al. A polymorphism within IL21R confers risk for systemic lupus erythematosus. Arthritis Rheum 2009;60(8):2402–7.
[22] Niu X, He D, Zhang X, Yue T, Li N, Zhang JZ, et al. IL-21 regulates Th17 cells in rheumatoid arthritis. Hum Immunol 2010;71(4):334–41.
[23] Young DA, Hegen M, Ma HL, Whitters MJ, Albert LM, Lowe L, et al. Blockade of the interleukin-21/interleukin-21 receptor pathway ameliorates disease in animal models of rheumatoid arthritis. Arthritis Rheum 2007;56(4):1152–63.
[24] Herber D, Brown TP, Liang S, Young DA, Collins M, Dunussi-Joannopoulos K. IL-21 has a pathogenic role in a lupus-prone mouse model and its blockade with IL-21R. Fc reduces disease progression. J Immunol 2007;178(6):3822–30.
[25] Ding R, Gao W, He Z, Liao M, Wu F, Zou S, et al. Effect of serum interleukin 21 on the development of coronary artery disease. APMIS 2014;122(9):842–7.
[26] Hellings WE, Moll FL, de Vries JP, de Bruin P, de Kleijn DP, Pasterkamp G. Histological characterization of restenotic carotid plaques in relation to recurrence interval and clinical presentation: a cohort study. Stroke 2008;39(3):1029–32.
[27] Depuydt MAC, Prange KHM, Slenders L, Ord T, Elbersen D, Boltjes A, et al. Microanatomy of the human atherosclerotic plaque by single-cell transcriptomics. Circ Res 2020;127(11):1437–55.
[28] Smit V, de Mol J, Schaftenaar FH, Depuydt MAC, Postel RJ, Smeets D, et al. Single-cell profiling reveals age-associated immunity in atherosclerosis. Cardiovasc Res 2023;119(15):2508–21.
[29] Cochain C, Vafadarnejad E, Arampatzi P, Pelisek J, Winkels H, Ley K, et al. Single-cell RNA-seq reveals the transcriptional landscape and heterogeneity of aortic macrophages in murine atherosclerosis. Circ Res 2018;122(12):1661–74.
[30] Kuy S, Dua A, Desai SS, Rossi PJ, Seabrook GR, Lewis BD, et al. Carotid endarterectomy national trends over a decade: does sex matter? Ann Vasc Surg 2014;28(4):887–92.
[31] Smit V, de Mol J, Kleijn M, Depuydt MAC, de Winther MPJ, Bot I, et al. Sexual dimorphism in atherosclerotic plaques of aged Ldlr(-/-) mice. Immun Ageing 2024;21(1):27.
[32] Agrawal A, Su H, Chen J, Osann K, Agrawal S, Gupta S. Increased IL-21 secretion by aged CD4+T cells is associated with prolonged STAT-4 activation and CMV seropositivity. Aging (Albany NY) 2012;4(9):648–59.
[33] Oyamada H, Ying Y, Agrawal S, Liu A, Subramanian VS, de Melo Bento CA, Agrawal A. Chronic IL-21 drives neuroinflammation and promotes lipid accumulation in microglia. Immun Ageing 2025;22(1):15.
[34] Zhou M, Zou R, Gan H, Liang Z, Li F, Lin T, et al. The effect of aging on the frequency, phenotype and cytokine production of human blood CD4 + CXCR5 + T follicular helper cells: comparison of aged and young subjects. Immun Ageing 2014;11:12.
[35] Nidorf SM, Eikelboom JW, Budgeon CA, Thompson PL. Low-dose colchicine for secondary prevention of cardiovascular disease. J Am Coll Cardiol 2013;61(4):404–10.
[36] Douna H, Amersfoort J, Schaftenaar FH, Kroner MJ, Kiss MG, Slutter B, et al. B- and T-lymphocyte attenuator stimulation protects against atherosclerosis by regulating follicular B cells. Cardiovasc Res 2020;116(2):295–305.
[37] Grievink HW, Smit V, Verwilligen RAF, Bernabe Kleijn MNA, Smeets D, Binder CJ, et al. Stimulation of the PD-1 pathway decreases atherosclerotic lesion development in Ldlr deficient mice. Front Cardiovasc Med 2021;8:740531.
[38] Ridker PM, Devalaraja M, Baeres FM, Engelmann MD, Hovingh GK, Ivkovic M, et al. IL-6 inhibition with ziltivekimab in patients at high atherosclerotic risk (RESCUE): a double-blind, randomised, placebo-controlled, phase 2 trial. Lancet 2021;397(10289):2060–9.
[39] Lee JH, Lydon JP, Kim CH. Progesterone suppresses the mTOR pathway and promotes generation of induced regulatory T cells with increased stability. Eur J Immunol 2012;42(10):2683–96.
[40] Polanczyk MJ, Carson BD, Subramanian S, Afentoulis M, Vandenbark AA, Ziegler SF, Offner H. Cutting edge: estrogen drives expansion of the CD4+CD25+ regulatory T cell compartment. J Immunol 2004;173(4):2227–30.
[41] Monteiro C, Kasahara T, Sacramento PM, Dias A, Leite S, Silva VG, et al. Human pregnancy levels of estrogen and progesterone contribute to humoral immunity by activating T(FH)/B cell axis. Eur J Immunol 2021;51(1):167–79.
[42] Petrelli A, Carvello M, Vergani A, Lee KM, Tezza S, Du M, et al. IL-21 is an antitolerogenic cytokine of the late-phase alloimmune response. Diabetes 2011;60(12):3223–34.
[43] Nian Y, Xiong Z, Zhan P, Wang Z, Xu Y, Wei J, et al. IL-21 Receptor Blockade Shifts the Follicular T Cell Balance and Reduces De Novo Donor-Specific Antibody Generation. Front Immunol 2021;12:661580.
[44] Bucher C, Koch L, Vogtenhuber C, Goren E, Munger M, Panoskaltsis-Mortari A, et al. IL-21 blockade reduces graft-versus-host disease mortality by supporting inducible T regulatory cell generation. Blood 2009;114(26):5375–84.
[45] Wan CK, Andraski AB, Spolski R, Li P, Kazemian M, Oh J, et al. Opposing roles of STAT1 and STAT3 in IL-21 function in CD4+ T cells. Proc Natl Acad Sci U S A 2015;112(30):9394–9.
[46] Laurence A, Amarnath S, Mariotti J, Kim YC, Foley J, Eckhaus M, et al. STAT3 transcription factor promotes instability of nTreg cells and limits generation of iTreg cells during acute murine graft-versus-host disease. Immunity 2012;37(2):209–22.
[47] Xu L, Kitani A, Stuelten C, McGrady G, Fuss I, Strober W. Positive and negative transcriptional regulation of the Foxp3 gene is mediated by access and binding of the Smad3 protein to enhancer I. Immunity 2010;33(3):313–25.
[48] Dietel B, Cicha I, Voskens CJ, Verhoeven E, Achenbach S, Garlichs CD. Decreased numbers of regulatory T cells are associated with human atherosclerotic lesion vulnerability and inversely correlate with infiltrated mature dendritic cells. Atherosclerosis 2013;230(1):92–9.
[49] Mor A, Luboshits G, Planer D, Keren G, George J. Altered status of CD4(+)CD25(+) regulatory T cells in patients with acute coronary syndromes. Eur Heart J 2006;27(21):2530–7.
[50] Potekhina AV, Pylaeva E, Provatorov S, Ruleva N, Masenko V, Noeva E, et al. Treg/Th17 balance in stable CAD patients with different stages of coronary atherosclerosis. Atherosclerosis 2015;238(1):17–21.
[51] Chauhan SK, Saban DR, Lee HK, Dana R. Levels of Foxp3 in regulatory T cells reflect their functional status in transplantation. J Immunol 2009;182(1):148–53.
[52] Klingenberg R, Gerdes N, Badeau RM, Gistera A, Strodthoff D, Ketelhuth DF, et al. Depletion of FOXP3+ regulatory T cells promotes hypercholesterolemia and atherosclerosis. J Clin Investig 2013;123(3):1323–34.

[53] Wang ZX, Lin J, Chen B, He SL, Ma XM, Li DZ. Effects of FOXP3 on the progression of atherosclerosis plaque in ApoE-knock out mice. Chinese Journal of Cellular and Molecular Immunology 2011;27(2):154–7.
[54] Mor A, Planer D, Luboshits G, Afek A, Metzger S, Chajek-Shaul T, et al. Role of naturally occurring CD4+ CD25+ regulatory T cells in experimental atherosclerosis. Arterioscler Thromb Vasc Biol 2007;27(4):893–900.
[55] Foks AC, Frodermann V, ter Borg M, Habets KL, Bot I, Zhao Y, et al. Differential effects of regulatory T cells on the initiation and regression of atherosclerosis. Atherosclerosis 2011;218(1):53–60.
[56] Sriranjan-Rothwell RS, Zhao TX, Hoole SP, Bond SJ, Tarkin JM, Brubert J, et al. Anti-inflammatory therapy with low-dose IL-2 in acute coronary syndromes: a randomized phase 2 trial. Nat Med 2026;32(2):624–32.
[57] Foks AC, Lichtman AH, Kuiper J. Treating atherosclerosis with regulatory T cells. Arterioscler Thromb Vasc Biol 2015;35(2):280–7.
[58] Mostafa Mtairag E, Chollet-Martin S, Oudghiri M, Laquay N, Jacob MP, Michel JB, Feldman LJ. Effects of interleukin-10 on monocyte/endothelial cell adhesion and MMP-9/TIMP-1 secretion. Cardiovasc Res 2001;49(4):882–90.
[59] Lin J, Li M, Wang Z, He S, Ma X, Li D. The role of CD4+CD25+ regulatory T cells in macrophage-derived foam-cell formation. J Lipid Res 2010;51(5):1208–17.
[60] Swirski FK, Nahrendorf M. Leukocyte behavior in atherosclerosis, myocardial infarction, and heart failure. Science 2013;339(6116):161–6.
[61] Moore KJ, Sheedy FJ, Fisher EA. Macrophages in atherosclerosis: a dynamic balance. Nat Rev Immunol 2013;13(10):709–21.
[62] Vallieres F, Durocher I, Girard D. Biological activities of interleukin (IL)-21 in human monocytes and macrophages. Cell Immunol 2019;337:62–70.
[63] Vallières F, Girard D. IL-21 enhances phagocytosis in mononuclear phagocyte cells: identification of spleen tyrosine kinase as a novel molecular target of IL-21. J Immunol 2013;190(6):2904–12.
[64] Xu M, Liu M, Du X, Li S, Li H, Li X, et al. Intratumoral delivery of IL-21 overcomes anti-Her2/Neu resistance through shifting tumor-associated macrophages from M2 to M1 phenotype. J Immunol 2015;194(10):4997–5006.
[65] Levack RC, Newell KL, Popescu M, Cabrera-Martinez B, Winslow GM. CD11c(+) T-bet(+) B cells require IL-21 and IFN-gamma from type 1 T follicular helper cells and intrinsic Bcl-6 expression but develop normally in the absence of T-bet. J Immunol 2020;205(4):1050–8.
[66] Wang S, Wang J, Kumar V, Karnell JL, Naiman B, Gross PS, et al. IL-21 drives expansion and plasma cell differentiation of autoreactive CD11c(hi)T-bet(+) B cells in SLE. Nat Commun 2018;9(1):1758.
[67] Pinderski LJ, Fischbein MP, Subbanagounder G, Fishbein MC, Kubo N, Cheroutre H, et al. Overexpression of interleukin-10 by activated T lymphocytes inhibits atherosclerosis in LDL receptor-deficient Mice by altering lymphocyte and macrophage phenotypes. Circ Res 2002;90(10):1064–71.
[68] Mallat Z, Besnard S, Duriez M, Deleuze V, Emmanuel F, Bureau MF, et al. Protective role of interleukin-10 in atherosclerosis. Circ Res 1999;85(8):e17–24.
[69] Caligiuri G, Rudling M, Ollivier V, Jacob MP, Michel JB, Hansson GK, Nicoletti A. Interleukin-10 deficiency increases atherosclerosis, thrombosis, and low-density lipoproteins in apolipoprotein E knockout mice. Mol Med 2003;9(1–2):10–7.
[70] Zotos D, Coquet JM, Zhang Y, Light A, D'Costa K, Kallies A, et al. IL-21 regulates germinal center B cell differentiation and proliferation through a B cell-intrinsic mechanism. J Exp Med 2010;207(2):365–78.
[71] Rankin AL, MacLeod H, Keegan S, Andreyeva T, Lowe L, Bloom L, et al. IL-21 receptor is critical for the development of memory B cell responses. J Immunol 2011;186(2):667–74.
[72] Kotlarz D, Zietara N, Uzel G, Weidemann T, Braun CJ, Diestelhorst J, et al. Loss-of-function mutations in the IL-21 receptor gene cause a primary immunodeficiency syndrome. J Exp Med 2013;210(3):433–43.
[73] Ignatenko S, Skrumsager BK, Mouritzen U. Safety, PK, and PD of recombinant anti-interleukin-21 monoclonal antibody in a first-in-human trial. Int J Clin Pharmacol Ther 2016;54(4):243–52.
[74] Hussaini A, Mukherjee R, Berdieva DM, Glogowski C, Mountfield R, Ho PTC. A double-blind, phase I, single ascending dose study to assess the safety, pharmacokinetics, and pharmacodynamics of BOS161721 in healthy subjects. Clin Transl Sci 2020;13(2):337–44.